Kinetic stability and reactivity of silicon and fluorine-containing CL-20 derivatives

Konstantin P. Katin[1] | **Masoud Bezi Javan[2]** | **Alexey I. Kochaev[3]** | **Alireza Soltani[4]** | **Mikhail M. Maslov[5]**

[1]Nanoengineering in Electronics, Spintronics and Photonics Institute, National Research Nuclear University "MEPhI", Kashirskoe Shosse 31, Moscow 115409, Russia

[2]Physics Department, Faculty of Sciences, Golestan University, Gorgan, Iran

[3]Department of Physics, Ulyanovsk State Technical University, Severny Venets str. 32, Ulyanovsk 432027, Russia

[4]Golestan Rheumatology Research Center, Golestan University of Medical Science, Gorgan, Iran

[5]Nanoengineering in Electronics, Spintronics and Photonics Institute, National Research Nuclear University "MEPhI", Kashirskoe Shosse 31, Moscow 115409, Russia

Correspondence
Author One PhD, Department, Institution, City, State or Province, Postal Code, Country
Email: correspondingauthor@email.com

Present address
Department, Institution, City, State or Province, Postal Code, Country

CL-20 based cages in which carbon/oxygen atoms are replaced by silicon/fluorine ones are studied using the ab initio molecular dynamics, density functional theory, and time-dependent density functional theory. In contrast to the pristine CL-20, the first step of pyrolysis of these cages is the migration of oxygen/fluorine atoms to silicon. Molecules containing fluorine are unstable at room temperature. The high-energy silicon-containing molecule ($CSi_5H_6N_{12}O_{12}$) is approximately as stable as pristine CL-20. Energy barrier preventing its decomposition is about 200 kJ/mol. Energies of the frontier orbitals and reactivity descriptors of $CSi_5H_6N_{12}O_{12}$ are very close to the corresponding values of pure CL-20. All studied cages can form covalent dimers via the methylene molecular bridges. It is found that the reactions of dimerization are exothermic. Dimers' isomers in which silicon atoms are located closer to the methylene bridges possess lower internal energies. It is found that the mechanisms of dimers' thermal decomposition are similar to the analog mechanisms of corresponding monomers. Dimerization of the cages results in the redshifts of their ultraviolet spectra.

Keywords —hexanitrohexaazaisowurtzitane, HNIW, pyrolysis mechanism, ab initio molecular dynamics, transition

state, dimers

Introduction

Hexanitrohexaazaisowurtzitane (HNIW), well-known as CL-20, is one of the most powerful high-energy molecules.[26] Like octogen (HMX) and hexogen (RDX), CL-20 belongs to the class of the nitroamine explosives. Due to its strained carbon-nitrogen skeleton with six attached nitro groups, CL-20 possesses much higher performance than HMX.[30] CL-20 was firstly synthesized from benzylamine and glyoxal in 1987 and began to be produced industrially from the 1990-s.[31] CL-20 can be obtained in both gaseous and condensed phases. Five different phases of solid CL-20, known as α, β, γ, ε, and ζ modifications, are possible.[27, 33] All of them are the molecular crystals with the weak van-der-Waals bonds between the CL-20 molecules. However, ε modification is the most stable under normal conditions.[6]

With regard to the practical importance of CL-20, there were many efforts to improve its properties (density, power, detonation velocity, sensitivity, etc.). The most suitable way to do this is co-crystallization of CL-20 with the other high-energy molecules that can fill hollows between isolated CL-20s. Co-crystals of CL-20 with HMX,[3] caprolactam,[9] MDNT,[1] DNT,[22] TNT,[19] TATB,[37] DNDAP,[23] and other compounds were recently prepared and characterized. All of them demonstrate some advantages over the pristine CL-20. Liu *et.al.* presented systematic consideration of different co-crystals based on CL-20.[21]

There are some alternative ways to improve the CL-20 properties. One of them is the use of substitutional derivatives of CL-20, in which one or more carbon atoms are replaced by silicon.[32] Silicon is placed in the same column of the periodic table as carbon and, therefore, possesses similar properties. Many carbon compounds have their silicon-substituted analogous. For example, silicon analogs of the high-energy pentaerythrityl tetraazide (PETN) were successfully synthesized.[15] They possess better sensitivity than the pristine carbon PETN.[24, 25] Another possibility for improving the CL-20 energy characteristics is to replace the NO_2 groups by NF_2 since fluorine demonstrates the higher oxidation activity than the oxygen. In addition, possible detonation product SiF4 has high negative formation enthalpy in comparison with SiO_2.[32] Tan *et.al.* presented an extensive computational study of all possible CL-20 derivatives containing silicon and fluorine.[32] According to these calculations, some derivatives possess higher crystalline densities, decomposition reaction heats, detonation velocities, detonation pressures and explosion temperatures, than the pristine CL-20 (for example, heat of decomposition of unsubstituted CL-20 and its silicon derivative $CSi_5H_6N_{12}O_{12}$ at constant volume are equal to -3241.6 and -5045.3 kJ/mol, respectively). Both pristine and substituted CL-20s do not have dangling bonds and, therefore, can not form covalent bonds with each other. However, they presumably can form covalent complexes via the methylene "molecular bridges" after detaching several nitro groups.[4] *Ab initio* calculations confirm that dimers and larger covalent complexes based on CL-20 molecules are stable, and their stability increases with the effective size of the system.[12, 7] Such complexes have higher densities in comparison with the molecular crystals due to the shorter distances between the CL-20 cages.

Here we present the computational study of CL-20 derivatives containing silicon and fluorine atoms. The mechanisms of their pyrolysis are studied using the *ab initio* molecular dynamics and potential energy surfaces investigations. In addition, we study in detail the structure, reactivity and optical spectra of the corresponding dimers in which two cages are attached to each other through the methylene molecular bridges.

MATERIALS AND METHODS

We consider three molecules in this study: $C_6H_6N_{12}O_{12}$ (pristine CL-20) and its two substituted derivatives, $CSi_5H_6N_{12}O_{12}$ and $C_4Si_2H_6N_{12}F_{12}$. Their atomic structures are presented in Fig. 1.
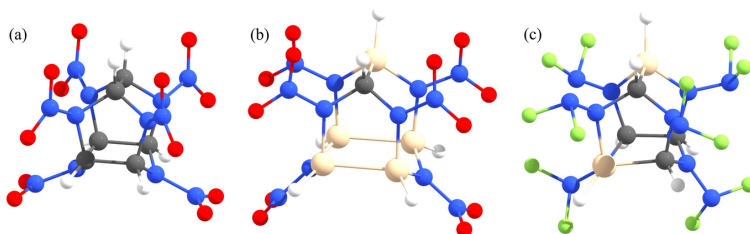

FIGURE 1 Atomic structures of $C_6H_6N_{12}O_{12}$ (CL-20) (a) and its substituted derivatives $CSi_5H_6N_{12}O_{12}$ (b) and $C_4Si_2H_6N_{12}F_{12}$ (c). Gray, blue, red, white, brown and green circles correspond to carbon, nitrogen, oxygen, hydrogen, silicon and fluorine atoms, respectively.

These derivatives were chosen because they demonstrate the highest heats of decomposition reactions, detonation velocities, and temperatures among all the other compounds.[32] Corresponding dimers are constructed using the methylene molecular bridges because methylene provides stronger binding than the other possible bridges.[4] Ground state geometries are optimized in the frame of density functional theory with the Becke's three-parameter functional B3LYP.[18, 2] Two electron basis sets 6-311G(d,p)[17] and 6-311G++(2d,2p)[5, 29] are used. Both of them result in almost the same energies, geometries, and frontier electronic orbitals. Thus, we use the smaller basis 6-311G(d,p) during the molecular dynamics run, hessian calculations, transition state search, and optical spectra computing. Terachem software[34, 35, 14, 8] which provides the high-performance quantum chemical algorithms on graphical processors is used for most calculations. GAMESS program package[28] is also applied for the local search of transition states and their validations.

Pyrolysis mechanisms are studied using the *ab initio* molecular dynamics at constant temperature T = 3000 K with the Langevin thermostat. Total simulation time is equal to 2 ps, whereas the time step is equal to 0.1 fs. Ten independent simulations were performed for each system. Decomposition paths adopted from the molecular dynamics were optimized in the frame of nudged elastic band (NEB) technique as it was implemented in TeraChem. Configurations with the highest energies on the NEB paths were additionally optimized using the Hessian-based local algorithm for the transition state search as it was implemented in GAMESS. Hessian calculations and an intrinsic reaction coordinate approach are carried out to confirm the transition state configuration. To take into account the influence of vibrational energies on pyrolysis mechanisms, we consider the Gibbs energies G for reactants, products and transition state configurations. Taking into account the ideal gas approximation, we evaluate Gibbs energy as

$G = E + E_{vib} + RT - TS_{vib}$,

where E and E_{vib} are the ground state and vibrational energies, respectively, S_{vib} is the vibrational entropy, R = 8.31 J/(mol·K) is the gaseous constant, T is the temperature.

Electron affinities (EA) and ionization potentials (IA) of considered compounds are calculated from their HOMO

and LUMO energies in accordance with the Koopmans' theorem for the closed-shell molecular systems.[16] Descriptors of reactivity, such as chemical hardness (η) and softness (S), the chemical potential (μ), electronegativity (χ) and electrophilicity index (ω), are determined by the same way as it was made in Ref. [7]. To calculate the ultraviolet (UV) spectra, all geometries were reoptimized with the CAM-B3LYP functional,[38] which took into account the long-range Coulomb correlations. Twenty excited states were found using the same CAM-B3LYP approach in the frame of Tamm-Dancoff time-dependent density functional technique implemented in TeraChem.[11]

RESULTS AND DISCUSSIONS

| Pyrolysis mechanisms of the CL-20 derivatives

CL-20 is a highly strained metastable compound and, therefore, it decomposes at high temperatures with a heat releasing. According to the previous studies, decomposition of CL-20 starts with the fission of nitro group that induces a skeleton destabilization and further decomposition.[10] So, the NO_2 fission determines the overall activation barrier.[10] The $N-NO_2$ bond dissociation is a barrierless process, and the corresponding bond dissociation energy needed for the NO_2 fission is about 200 kJ/mol.[20] In Ref. [32] the authors proposed a natural assumption that the same mechanism (NO_2 or NF_2 fission) is also relevant to the CL-20 derivatives. However, this assumption was not confirmed by our *ab initio* molecular dynamics simulations.

Observing the evolution of heated CL-20 derivatives, we found two competitive mechanisms of the initial decomposition step. The first mechanism is the NO_2 or NF_2 fission, and the second one is a migration of O or F atom with the formation of Si–O or Si–F covalent bond. Migration is possible for the Si-containing CL-20 derivatives because silicon possesses a larger covalent radius (1.11 Å) than the carbon (0.76 Å). Corresponding energetic diagrams are presented in Fig. 2. For the $CSi_5H_6N_{12}O_{12}$ system, the barrier for the NO_2 fission is somewhat lower than that for the O migration. Therefore, the NO_2 fission mechanism prevails at room temperature. However, at higher temperatures, one should consider thermal corrections. For example, at T = 3000 K (it is about the half of CL-20 explosive temperature) O migration mechanism becomes more feasible with regard to the lower Gibbs energy, as it is presented in Fig. 2a. Anyway, the energy barrier for the $CSi_5H_6N_{12}O_{12}$ decomposition is about 200 kJ/mol. This value is close to the corresponding value for the pristine CL-20.[20] Therefore, it can be said that $CSi_5H_6N_{12}O_{12}$ is as kinetically stable as pristine CL-20.

In contrast to oxygen, fluorine is able to easily migrate to the silicon atom and to destabilize the C4Si2H6N12F12 cage, see Fig. 2b. So, the C4Si2H6N12F12 system is much less stable. To evaluate its lifetime t before the decomposition, we adopt the Arrhenius formula

$$t = \left(\frac{1}{w} \right) \exp \left(-\frac{E_a}{kT} \right)$$

where w is the frequency factor, E_a is the activation energy, k is the Boltzmann's constant, T is the temperature. In our evaluation, we assume the activation energy is equal to the energy barrier (0.18 eV, see Fig. 2b). Frequency factor w can be defined from the Vineyard formula [36]

$$w = \frac{\Pi w_i}{\Pi w_i'} \quad .$$

Here ω and ω' are the real eigenfrequencies (normal modes) for the ground and transition states, respectively. Note that the numerator in this formula contains an additional factor because the transition state has one imaginary frequency, which is not taken into account. So, we obtain E_a = 0.18 eV and w = 1.93·10^{15} 1/s. In accordance with the Arrhenius formula, $t \sim 0.5$ ps at T = 300 K. So, $CSi_5H_6N_{12}O_{12}$ is unstable at room temperature and is barely suitable for practical applications.

We also stress the fact that the kinetic stability of any cage compound is determined by the energy barrier pre-

venting its decomposition rather than the strain energy enclosed in its framework. For example, methylcubanes demonstrate an inverse relationship between their strain energies and kinetic stabilities.[13] Moreover, initial processes leading to the CL-20 decomposition do not necessarily involve any framework transformation. For these reasons, cage strain energy is not a suitable measure of the stability of the CL-20 derivatives, as it is discussed in Ref. [32]. Although the CL-20 derivatives containing silicon possess higher strain energies,[32] they are not necessarily kinetically unstable.

| Dimers of the CL-20 derivatives

According to the previous studies,[4, 12] CL-20 molecules can form covalent dimers via the methylene molecular bridges (see Fig. 3a). Similar dimers can be constructed from the CL-20 derivatives. Dimers of $CSi_5H_6N_{12}O_{12}$ and $C_4Si_2H_6N_{12}F_{12}$ have three and eight possible isomers, respectively. These isomers differ from each other by the relative positions of silicon atoms. Structures of all isomers as well as their relative energies are presented in Fig. 3. One can see that the isomers in which carbon atoms are located far from the methylene bridges possess lower energies. This rule holds true for all dimers of both $CSi_5H_6N_{12}O_{12}$ and $C_4Si_2H_6N_{12}F_{12}$ systems. So, the presence of silicon close to the methylene bridges promotes the dimers formation. Unfavorable location of carbon atoms close to the methylene bridges results in increasing of internal energies by at least ~0.14 eV and ~0.32 eV for the dimers of $CSi_5H_6N_{12}O_{12}$ and $C_4Si_2H_6N_{12}F_{12}$, respectively. These values are much higher than the typical thermal energies kT (even at high temperature of 1000 K kT ~ 86 meV). So, the formation of unfavorable dimers is improbable.

Calculated HOMO and LUMO energies, as well as the quantum descriptors of reactivity for considered systems, are presented in Table 1.

Values obtained within the 6-311G++(2d,2p) and 6-311G(d,p) basis sets demonstrate good agreement, therefore, the smaller basis set is found to be sufficient for the CL-20 and its derivatives. CL-20 and $CSi_5H_6N_{12}O_{12}$ cages have almost the same energies of frontier orbitals and, therefore, possess rather similar chemical properties and reactivity. The presence of silicon atoms in the molecular framework does not change significantly the values of HOMO and LUMO energies since LUMO orbitals mainly concentrate on the nitro groups (see Fig. 4).

On the other hand, $C_4Si_2H_6N_{12}F_{12}$ and its dimers have much higher LUMO energies due to the presence of fluorine atoms. As a result, fluorine-containing cages possess higher HOMO-LUMO gaps and chemical hardness, and significantly lower electrophilicity. For all considered cages, dimers demonstrate lower HOMO-LUMO gaps and chemical hardness due to their large effective sizes. Such behavior is typical for the most cage-like molecules.

To evaluate the possible energy gain associated with the dimer formation, we consider hypothetical dimerization reaction in the following form

$2M + 2CH_2$ D + $4NX_2$ (X=O or F),
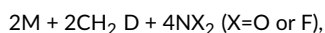
where M is a monomer (CL-20, $CSi_5H_6N_{12}O_{12}$ or $C_4Si_2H_6N_{12}F_{12}$), and D is the corresponding dimer. Thermodynamic characteristics of these reactions are calculated for the low-energy dimers as a difference between the corresponding values of energies and Gibbs energies for the products and reactants. Obtained data are presented in Table 2. Negative values of ΔE and ΔG show that the dimerization reaction is energetically favorable. High temperature inhibits dimerization, especially for the $CSi_5H_6N_{12}O_{12}$ cage. However, ΔG remains negative for all considered dimers even at very high temperature of 3000 K.

To gain further insight concerning the dimerization process, we calculate the binding energies (*BE*) between nitrogen atoms and methylene bridges. In every dimer, two monomers are linked together via four N–CH_2 bonds, see Fig. 3. The breaking of these bonds leads to the dimer separation into four fragments (two CH_2s and two cages). So, we define *BE* of N–CH_2 bonds as the quarter of energy difference between these fragments and entire dimer. Obtained *BE*s are also presented in Table 2. These values of *BE* are even higher than the value of *BE* calculated at the same level of theory for the CH_3–NH_2 molecule (4.20 eV). One can see that *BE*s for the Si-substituted dimers are significantly higher than the corresponding values for the CL-20 dimer. Therefore, Si-substituted cages possess a stronger connection with each other via the methylene bridges than the pristine CL-20s.

During the molecular dynamics simulation of heated dimers, we observe the same pyrolysis mechanisms as for the corresponding monomers (NO_2 fission and O/F migration to Si). We have never observed the contribution of methylene bridges to the initial decomposition step. So, we conclude that dimers are approximately as kinetically stable as the corresponding monomers.

| UV spectra of the CL-20 derivatives and their dimers

Optical spectra analysis is the common way for the experimental detection of dimerization of isolated CL-20 or its derivatives. According to our time-dependent density functional calculations, all considered cages, as well as their dimers, are not active in the visible range due to their hardness. However, they demonstrate an optical response in the UV range (150 ÷ 250 nm). UV spectra for the CL-20, $CSi_5H_6N_{12}O_{12}$, and $C_4Si_2H_6N_{12}F_{12}$ systems as well as for the corresponding low-energy dimers are presented in Fig. 5. Dimer formation leads to the redshifts on the spectra for all considered cages. This effect is expected with regard to larger effective sizes of dimers in comparison with monomers. The values of redshifts are 29, 25, and 18 nm for the CL-20, $CSi_5H_6N_{12}O_{12}$, and $C_4Si_2H_6N_{12}F_{12}$, respectively. These values are sufficient for the dimers formation detection using their spectral analysis.

CONCLUSION

Despite the impressive advances in preparing of co-crystals based on the CL-20 cages, we believe that co-crystallization is not the only way for improving the characteristics of CL-20. In particular, substituted CL-20 derivatives demonstrate some advantages over the pristine CL-20 and other nitroamine high-energy systems. Computer simulation is a cheap and suitable way for the selection of the most stable and powerful compounds among a wide variety of CL-20 derivatives. Efforts to synthesize new CL-20-like cages should be preceded by the comprehensive theoretical studies.

In the presented study, we consider pyrolysis mechanisms, stability, and reactivity of two promising silicon CL-20 derivatives as well as their dimers. We obtain that the presence of silicon atoms in the cage changes the mechanisms of initial pyrolysis step, but does not significantly reduce the stability of the cage. In addition, Si-containing cages are more prone to dimerization. On the other hand, the simultaneous presence of silicon and fluorine atoms results in the compound instability.

With regard to the presented results as well as the previously published data, the $CSi_5H_6N_{12}O_{12}$ compound seems to be the most attractive structure. It demonstrates higher crystalline densities, decomposition reaction heats, detonation velocities, detonation pressures, and explosion temperatures than the pristine CL-20.[32] At the same time, according to the presented results, its kinetic stability, frontier orbitals, and chemical reactivity is very similar to the CL-20 characteristics. The possibility of $CSi_5H_6N_{12}O_{12}$ synthesis from the silicon analogies of benzylamine and

glyoxal or other precursors is a rather difficult task, which requires particular consideration.

Acknowledgements

Conflict of interest

The authors declare that there is no conflict of interests regarding the publication of this paper.

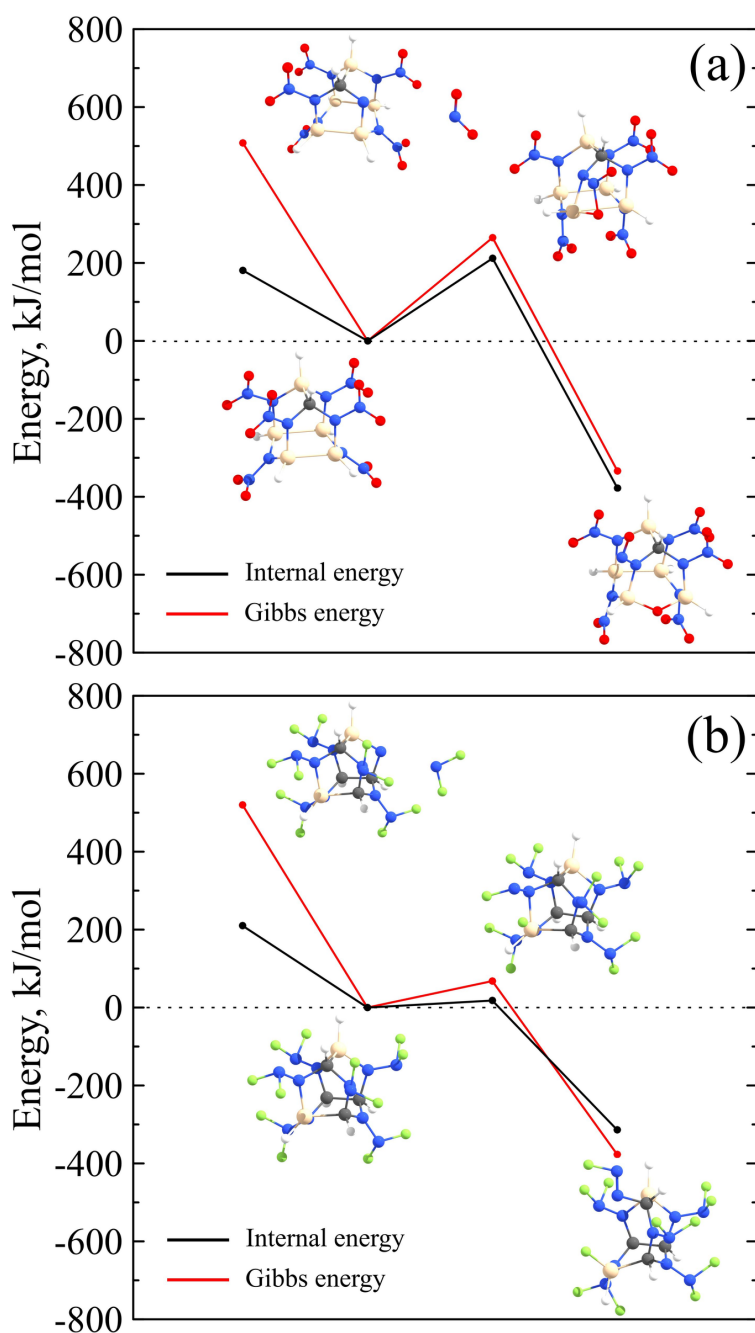**FIGURE 2** Two competitive mechanisms of $CSi_5H_6N_{12}O_{12}$ (a) and $C_4Si_2H_6N_{12}F_{12}$ (b) decomposition: NO_2/NF_2 fission versus O/F migration to Si. Black and red lines correspond to the internal energies and Gibbs energies at $T = 3000$ K, respectively. Optimized coordinates of stable and transition states are also available in Supplementary Materials.
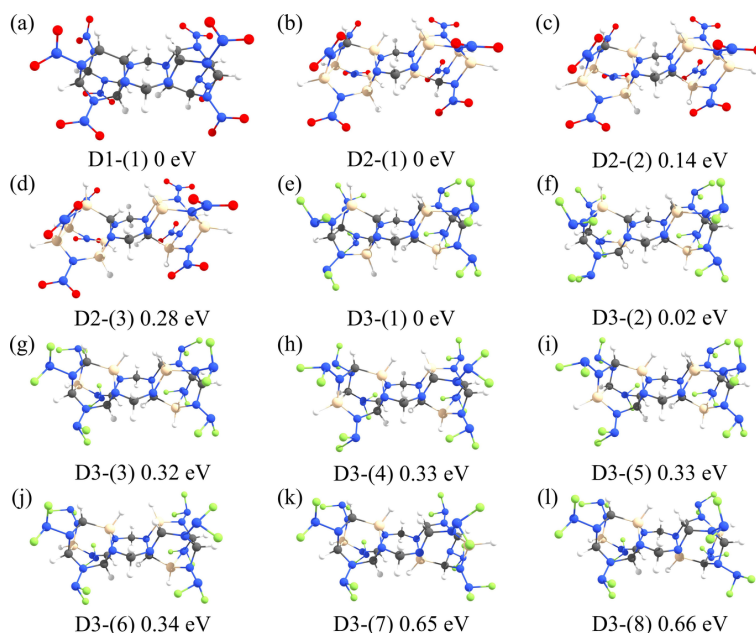
FIGURE 3 Covalent dimers of CL-20 (a), $CSi_5H_6N_{12}O_{12}$ (b) – (d) and $C_4Si_2H_6N_{12}F_{12}$ (e) – (l). The lowest energy dimers of CL-20, $CSi_5H_6N_{12}O_{12}$, and $C_4Si_2H_6N_{12}F_{12}$ are labeled as D1-(1), D2-(1), and D3-(1), respectively. Energy differences between every dimer and the corresponding low-energy dimer are presented in eV. Optimized coordinates of these compounds are also available in Supplementary Materials.
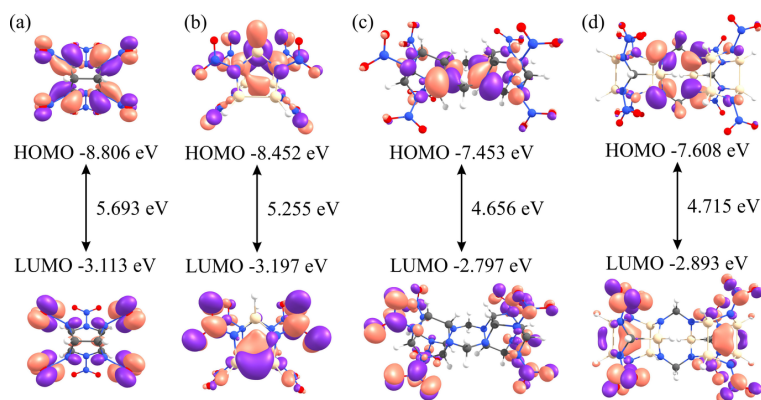

FIGURE 4 Frontier orbitals of CL-20 (a), $CSi_5H_6N_{12}O_{12}$ (b) as well as dimers D1-(1) (c) and D2-(1) (d).

Compound	ε_H	ε_L	Δ	μ	η	S	ω
Monomers							
CL-20	-8.99(-8.81)	-3.39(-3.11)	5.61(5.69)	-6.19(-5.96)	2.8(2.85)	0.18(0.18)	6.83(6.24)
$CSi_5H_6N_{12}O_{12}$	-8.58(-8.45)	-3.48(-3.2)	5.1(5.25)	-6.03(-5.82)	2.55(2.63)	0.2(0.19)	7.13(6.46)
$C_4Si_2H_6N_{12}F_{12}$	-8.29(-8.06)	-2.06(-1.67)	6.23(6.39)	-5.18(-4.87)	3.11(3.19)	0.16(0.16)	4.3(3.71)
Dimers							
D1-(1)	-7.64(-7.45)	-3.06(-2.79)	4.58(4.66)	-5.35(-5.12)	2.29(2.33)	0.22(0.21)	6.24(5.64)
D2-(1)	-7.79(-7.63)	-3.15(-2.89)	4.64(4.74)	-5.47(-5.26)	2.32(2.37)	0.22(0.21)	6.46(5.84)
D2-(2)	-7.62(-7.49)	-3.27(-3.03)	4.35(4.46)	-5.45(-5.26)	2.18(2.23)	0.23(0.22)	6.82(6.21)
D2-(3)	-7.58(-7.48)	-3.26(-3.02)	4.32(4.46)	-5.42(-5.25)	2.16(2.23)	0.23(0.22)	6.81(6.17)
D3-(1)	-7.39(-7.18)	-1.85(-1.49)	5.54(5.69)	-4.62(-4.34)	2.77(2.84)	0.18(0.18)	3.85(3.3)
D3-(2)	-7.46(-7.25)	-1.83(-1.45)	5.63(5.8)	-4.65(-4.35)	2.81(2.9)	0.18(0.17)	3.84(3.27)
D3-(3)	-7.41(-7.17)	-1.86(-1.49)	5.55(5.68)	-4.64(-4.33)	2.78(2.84)	0.18(0.18)	3.87(3.3)
D3-(4)	-7.41(-7.15)	-1.87(-1.46)	5.54(5.69)	-4.64(-4.31)	2.77(2.84)	0.18(0.18)	3.89(3.26)
D3-(5)	-7.31(-7.08)	-1.82(-1.45)	5.49(5.63)	-4.56(-4.26)	2.75(2.82)	0.18(0.18)	3.79(3.23)
D3-(6)	-7.37(-7.11)	-1.87(-1.47)	5.49(5.64)	-4.62(-4.29)	2.75(2.82)	0.18(0.18)	3.88(3.27)
D3-(7)	-7.3(-7.05)	-1.88(-1.49)	5.41(5.55)	-4.59(-4.27)	2.71(2.78)	0.18(0.18)	3.89(3.28)
D3-(8)	-7.25(-6.98)	-1.88(-1.49)	5.37(5.49)	-4.57(-4.24)	2.69(2.74)	0.19(0.18)	3.89(3.27)

TABLE 1 . Electronic properties and descriptors of reactivity for CL-20 derivatives and their dimers. HOMO energy εH (eV), LUMO energy ε_L (eV), HOMO-LUMO gap $\Delta = \varepsilon_H - \varepsilon_L$ (eV), chemical potential $\mu = (\varepsilon_H + \varepsilon_L)/2$ (eV), chemical hardness $\eta = \Delta/2$ (eV) and softness $S = 1/(2\eta)$ (eV^{-1}) as well as electrophilicity $\omega = \mu^2/(2\eta)$ are presented for every compound (see Ref. [7] and references wherein for the information about chemical descriptors). Values are calculated using the 6-311G++(2d,2p) basis set, whereas values in parenthesis are calculated using the smaller 6-311G(d,p) basis set. .

Dimer	ΔE	ΔG (300 K)	ΔG (3000 K)	BE
D1-(1)	-8.61	-812.0	-260.6	4.39
D2-(1)	-8.32	-771.6	-68.5	4.97
D3-(1)	-8.4	-786.1	-143.8	4.73

TABLE 2 . Energies (ΔE, eV) and Gibbs energies (ΔG, kJ/mol) of dimerization reactions 2M + 2CH$_2$ D + 4NX$_2$ (X=O or F; M = monomer CL-20, CSi$_5$H$_6$N$_{12}$O$_{12}$ or C$_4$Si$_2$H$_6$N$_{12}$F$_{12}$; D is the corresponding low-energy dimer, presented in Fig. 3). Binding energies (*BE*, eV) for the N–CH$_2$ bonds in the dimers are also presented. .
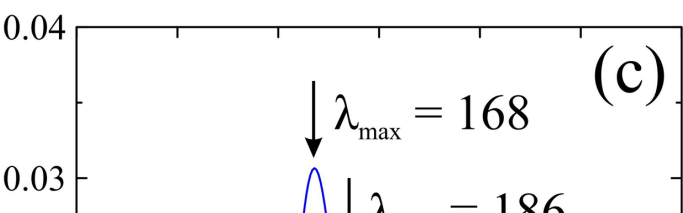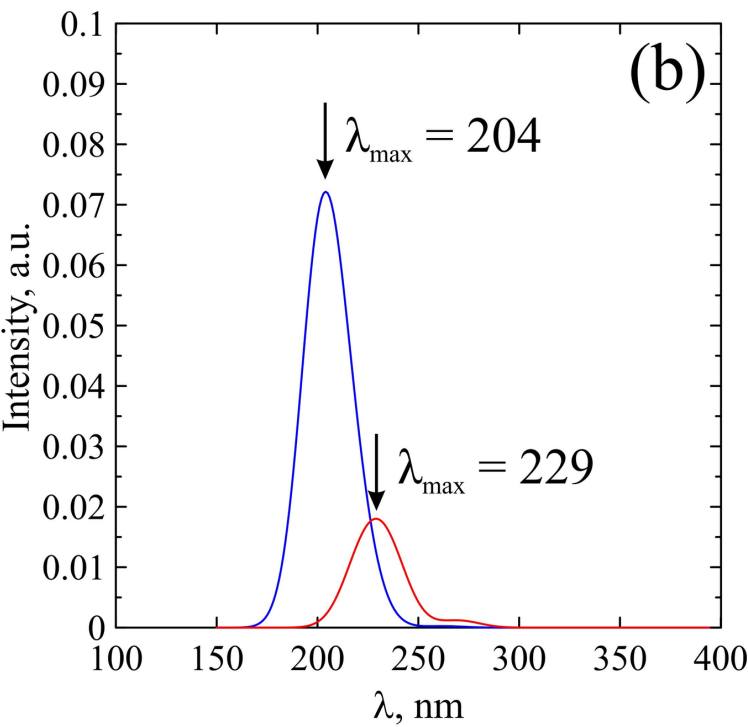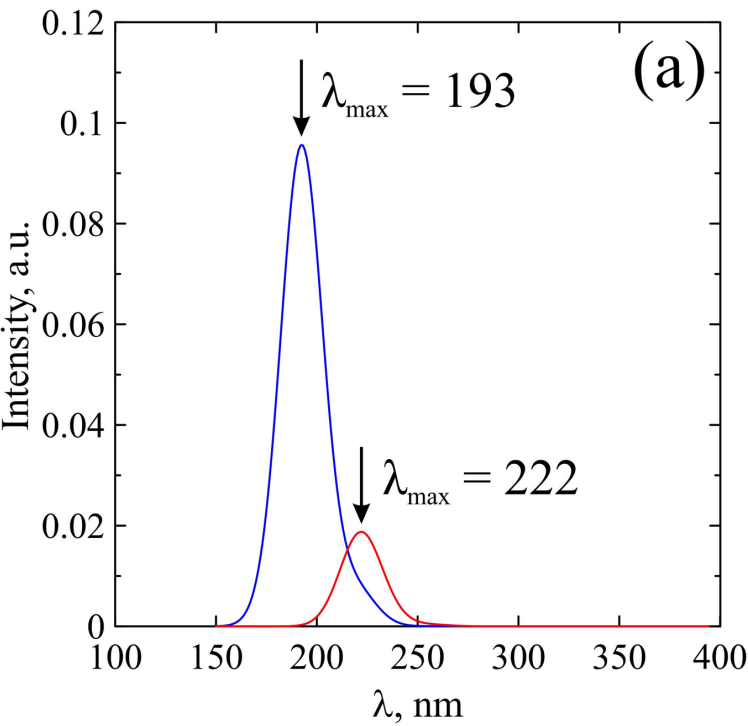
References

[1] Stephen R. Anderson, Pascal Dubé, Mariusz Krawiec, Jerry S. Salan, David J. am Ende, and Philip Samuels. Promising CL-20-Based Energetic Material by Cocrystallization. *Propellants Explosives, Pyrotechnics*, 41(5):783–788, aug 2016.

[2] Axel D. Becke. Density-functional thermochemistry. III. The role of exact exchange. *The Journal of Chemical Physics*, 98(7):5648–5652, apr 1993.

[3] Onas Bolton, Leah R. Simke, Philip F. Pagoria, and Adam J. Matzger. High Power Explosive with Good Sensitivity: A 2:1 Cocrystal of CL-20:HMX. *Crystal Growth & Design*, 12(9):4311–4314, aug 2012.

[4] N. N. Degtyarenko, K. P. Katin, and M. M. Maslov. Simulation of metastable CL-20 cluster structures. *Physics of the Solid State*, 56(7):1467–1471, jul 2014.

[5] David Feller. The role of databases in support of computational chemistry calculations. *Journal of Computational Chemistry*, 17(13):1571–1586, oct 1996.

[6] M. Frances Foltz, Clifford L. Coon, Frank Garcia, and Albert L. Nichols. The thermal stability of the polymorphs of hexanitrohexaazaisowurtzitane Part I. *Propellants, Explosives, Pyrotechnics*, 19(1):19–25, feb 1994.

[7] Margarita A. Gimaldinova, Mikhail M. Maslov, and Konstantin P. Katin. Electronic and reactivity characteristics of CL-20 covalent chains and networks: a density functional theory study. *CrystEngComm*, 20(30):4336–4344, 2018.

[8] T. P. M. Goumans, C. Richard A. Catlow, Wendy A. Brown, Johannes Kästner, and Paul Sherwood. An embedded cluster study of the formation of water on interstellar dust grains. *Physical Chemistry Chemical Physics*, 11(26):5431, 2009.

[9] Changyan Guo, Haobin Zhang, Xiaochuan Wang, Jinjiang Xu, Yu Liu, Xiaofeng Liu, Hui Huang, and Jie Sun. Crystal structure and explosive performance of a new CL-20/caprolactam cocrystal. *Journal of Molecular Structure*, 1048:267–273, sep 2013.

[10] Olexandr Isayev, Leonid Gorb, Mo Qasim, and Jerzy Leszczynski. Ab Initio Molecular Dynamics Study on the Initial Chemical Events in Nitramines: Thermal Decomposition of CL-20. *The Journal of Physical Chemistry B*, 112(35):11005–11013, sep 2008.

[11] Christine M. Isborn, Nathan Luehr, Ivan S. Ufimtsev, and Todd J. Martínez. Excited-State Electronic Structure with Configuration Interaction Singles and Tamm–Dancoff Time-Dependent Density Functional Theory on Graphical Processing Units. *Journal of Chemical Theory and Computation*, 7(6):1814–1823, may 2011.

[12] Konstantin P. Katin and Mikhail M. Maslov. Toward CL-20 crystalline covalent solids: On the dependence of energy and electronic properties on the effective size of CL-20 chains. *Journal of Physics and Chemistry of Solids*, 108:82–87, sep 2017.

[13] Konstantin P. Katin, Vladimir S. Prudkovskiy, and Mikhail M. Maslov. Influence of methyl functional groups on the stability of cubane carbon cage. *Physica E: Low-dimensional Systems and Nanostructures*, 81:1–6, jul 2016.

[14] Johannes Kastner, Joanne M. Carr, Thomas W. Keal, Walter Thiel, Adrian Wander, and Paul Sherwood. DL-FIND: An Open-Source Geometry Optimizer for Atomistic Simulations†. *The Journal of Physical Chemistry A*, 113(43):11856–11865, oct 2009.

[15] Thomas M. Klapötke, Burkhard Krumm, Rainer Ilg, Dennis Troegel, and Reinhold Tacke. The Sila-Explosives Si(CH2N3)4 and Si(CH2ONO2)4: Silicon Analogues of the Common Explosives Pentaerythrityl Tetraazide C(CH2N3)4, and Pentaerythritol Tetranitrate, C(CH2ONO2)4. *Journal of the American Chemical Society*, 129(21):6908–6915, may 2007.

[16] T Koopmans. Über die Zuordnung von Wellenfunktionen und Eigenwerten zu den Einzelnen Elektronen Eines Atoms. *Physica*, 1(1-6):104–113, jan 1934.

[17] R. Krishnan, J. S. Binkley, R. Seeger, and J. A. Pople. Self-consistent molecular orbital methods. XX. A basis set for correlated wave functions. *The Journal of Chemical Physics*, 72(1):650–654, jan 1980.

[18] Chengteh Lee, Weitao Yang, and Robert G. Parr. Development of the Colle-Salvetti correlation-energy formula into a functional of the electron density. *Physical Review B*, 37(2):785–789, jan 1988.

[19] Huarong Li, Yuanjie Shu, Shijie Gao, Ling Chen, Qing Ma, and Xuehai Ju. Easy methods to study the smart energetic TNT/CL-20 co-crystal. *Journal of Molecular Modeling*, 19(11):4909–4917, sep 2013.

[20] Liu Lin-lin and Song qi Hu. Ab initio calculations of the NO2 fission for CL-20 conformers. *Journal of Energetic Materials*, pages 1–8, nov 2018.

[21] Guangrui Liu, Hongzhen Li, Ruijun Gou, and Chaoyang Zhang. Packing Structures of CL-20-Based Cocrystals. *Crystal Growth & Design*, 18(11):7065–7078, oct 2018.

[22] Ke Liu, Gao Zhang, Jieyu Luan, Zhiqun Chen, Pengfei Su, and Yuanjie Shu. Crystal structure spectrum character and explosive property of a new cocrystal CL-20/DNT. *Journal of Molecular Structure*, 1110:91–96, apr 2016.

[23] Ning Liu, Binghui Duan, Xianming Lu, Hongchang Mo, Minghui Xu, Qian Zhang, and Bozhou Wang. Preparation of CL-20/DNDAP cocrystals by a rapid and continuous spray drying method: an alternative to cocrystal formation. *CrystEngComm*, 20(14):2060–2067, 2018.

[24] Wei-Guang Liu, Sergey V. Zybin, Siddharth Dasgupta, Thomas M. Klapotke, and William A. Goddard III. Explanation of the Colossal Detonation Sensitivity of Silicon Pentaerythritol Tetranitrate (Si-PETN) Explosive. *Journal of the American Chemical Society*, 131(22):7490–7491, jun 2009.

[25] Jane S. Murray, Pat Lane, Anian Nieder, Thomas M. Klapötke, and Peter Politzer. Enhanced detonation sensitivities of silicon analogs of PETN: reaction force analysis and the role of σ–hole interactions. *Theoretical Chemistry Accounts*, 127(4):345–354, jan 2010.

[26] U. R. Nair, R. Sivabalan, G. M. Gore, M. Geetha, S. N. Asthana, and H. Singh. Hexanitrohexaazaisowurtzitane (CL-20) and CL-20-based formulations (review). *Combustion Explosion, and Shock Waves*, 41(2):121–132, mar 2005.

[27] T. P. Russell, P. J. Miller, G. J. Piermarini, and S. Block. Pressure/temperature phase diagram of hexanitrohexaazaisowurtzitane. *The Journal of Physical Chemistry*, 97(9):1993–1997, mar 1993.

[28] Michael W. Schmidt, Kim K. Baldridge, Jerry A. Boatz, Steven T. Elbert, Mark S. Gordon, Jan H. Jensen, Shiro Koseki, Nikita Matsunaga, Kiet A. Nguyen, Shujun Su, Theresa L. Windus, Michel Dupuis, and John A. Montgomery. General atomic and molecular electronic structure system. *Journal of Computational Chemistry*, 14(11):1347–1363, nov 1993.

[29] Karen L. Schuchardt, Brett T. Didier, Todd Elsethagen, Lisong Sun, Vidhya Gurumoorthi, Jared Chase, Jun Li, and Theresa L. Windus. Basis Set Exchange: A Community Database for Computational Sciences. *Journal of Chemical Information and Modeling*, 47(3):1045–1052, apr 2007.

[30] R. L. Simpson, P. A. Urtiew, D. L. Ornellas, G. L. Moody, K. J. Scribner, and D. M. Hoffman. CL-20 performance exceeds that of HMX and its sensitivity is moderate. *Propellants Explosives, Pyrotechnics*, 22(5):249–255, oct 1997.

[31] Sergey V Sysolyatin, Antonina A Lobanova, Yuliya T Chernikova, and Gennady V Sakovich. Methods of synthesis and properties of hexanitrohexaazaisowurtzitane. *Russian Chemical Reviews*, 74(8):757–764, aug 2005.

[32] Bisheng Tan, Hui Huang, Ming Huang, Xinping Long, Jinshan Li, Xiaodong Yuan, and Ruijuan Xu. Computational screening of several silicon-based high-energy hexanitrohexaazaisowurtzitane-like derivatives. *Journal of Fluorine Chemistry*, 158:29–37, feb 2014.

[33] Jia-Jin Tan, Guang-Fu Ji, Xiang-Rong Chen, and Zhe Li. Structure equation of state and elasticity of crystalline HNIW by molecular dynamics simulations. *Physica B: Condensed Matter*, 406(15-16):2925–2930, aug 2011.

[34] Alexey V. Titov, Ivan S. Ufimtsev, Nathan Luehr, and Todd J. Martinez. Generating Efficient Quantum Chemistry Codes for Novel Architectures. *Journal of Chemical Theory and Computation*, 9(1):213–221, nov 2012.

[35] Ivan S. Ufimtsev and Todd J. Martinez. Quantum Chemistry on Graphical Processing Units. 3. Analytical Energy Gradients Geometry Optimization, and First Principles Molecular Dynamics. *Journal of Chemical Theory and Computation*, 5(10):2619–2628, aug 2009.

[36] George H. Vineyard. Frequency factors and isotope effects in solid state rate processes. *Journal of Physics and Chemistry of Solids*, 3(1-2):121–127, jan 1957.

[37] Haifeng Xu, Xiaohui Duan, Hongzhen Li, and Chonghua Pei. A novel high-energetic and good-sensitive cocrystal composed of CL-20 and TATB by a rapid solvent/non-solvent method. *RSC Advances*, 5(116):95764–95770, 2015.

[38] Takeshi Yanai, David P Tew, and Nicholas C Handy. A new hybrid exchange–correlation functional using the Coulomb-attenuating method (CAM-B3LYP). *Chemical Physics Letters*, 393(1-3):51–57, jul 2004.